Proceedings of GT2005
ASME Turbo Expo 2005: Power for Land, Sea and Air
June 6-9, 2005, Reno-Tahoe, Nevada, USA

Paper Number GT2005-68630

EVALUATION AND CHARACTERIZATION OF IRON- AND NICKEL-BASED ALLOYS FOR MICROTURBINE RECUPERATORS

Edgar Lara-Curzio, R. Trejo, K. L. More, P. J. Maziasz and B. A. Pint
Metals & Ceramics Division
Oak Ridge National Laboratory
Oak Ridge, TN 37831-6069

ABSTRACT

The effects of stress, temperature and time of exposure to microturbine exhaust gases on the mechanical properties and corrosion resistance of alloys HR-120® and 230® was investigated at turbine exhaust temperatures between 620°C and 760°C. It was found that the ultimate tensile strength and ductility of alloy 230® decreased by 30% and 60%, respectively, after 500 hours exposure at 752°C. At the lowest exposure temperature of 679°C the ultimate tensile strength and ductility decreased by 10% and 25%, respectively. The ultimate tensile strength and ductility of HR-120® alloy decreased by 15% and 50%, respectively, after 500 hours exposure at 745°C. At the lowest exposure temperature of 632°C the ultimate tensile strength and ductility decreased by 10% and 23%, respectively. The microstructural changes associated with exposure to microturbine exhaust gases are analyzed and discussed.

INTRODUCTION

The challenging performance targets for the next generation of microturbines include fuel-to-electricity efficiency of 40%, capital costs less than $500/kW, NOx emissions reduced to single parts per million, several years of operation between overhauls, life of 40,000 hours and fuel flexibility [1]. Significant increases in microturbine efficiency can be achieved by increasing engine-operating temperatures, and that can be realized through the use of advanced metallic alloys and ceramics for high-temperature components.

One of the critical components of low-compression ratio microturbines is the recuperator, which is responsible for a significant fraction of the overall efficiency of the microturbine [2]. Conventional recuperators are thin-sheet metallic heat exchangers that recover some of the waste heat from the exhaust stream and transfer it to the incoming air stream. The preheated incoming air is then used for combustion because less fuel is required to raise its temperature to the required level at the turbine inlet. Most of today's compact recuperators are manufactured using 300 series (e.g.- 347) stainless steels which are used at exhaust-gas temperatures below about 650° C [3]. At higher temperatures, these materials are susceptible to creep deformation and oxidation, which lead to structural deterioration and leaks, reducing the effectiveness and life of the recuperator. The temperature requirements for the next generation of microturbines have prompted efforts to screen and evaluate candidate materials with the required creep and corrosion resistance. Furthermore, developmental efforts will be needed to adapt current recuperator manufacturing processes to advanced alloys, to reduce costs, and enable long-term reliable operation at higher temperatures.

As part of a program sponsored by the U.S. Department of Energy to support microturbine manufacturers in the development of the next generation of microturbines, a recuperator test facility was established at Oak Ridge National Laboratory (ORNL) [4]. The objective of this test facility is to screen and evaluate candidate materials for microturbine recuperators inside a microturbine at turbine exit temperatures (TET) as high as 850°C. Furthermore, the preparation of

samples for these experiments, which requires welding test specimens to a sample holder, provides the means for identifying potential manufacturability barriers with a particular material.

In this paper the results from the evaluation of foils of alloy HR-120® and 230® alloy are presented after exposure in ORNL's microturbine recuperator testing facility for 500 hours at turbine exit temperatures as high as 785°C. The effect of exposure on the corrosion resistance and tensile strength and ductility and of the material is discussed and the results are compared to those for 347 stainless steel.

EXPERIMENTAL

In 2001, ORNL acquired a 60kW Capstone microturbine. In collaboration with Capstone Turbine Corp., the microturbine was modified to achieve higher TET values and to allow for the placement of test specimens, through six port bosses, at the entrance of the recuperator. Figure 1 shows a photograph of ORNL's microturbine recuperator testing facility and a schematic of the modified microturbine indicating the location of the port bosses with respect to the location of the radial recuperator. Further details of ORNL's microturbine recuperator testing facility can be found elsewhere [4-5].

The sample holder onto which the foils under evaluation are laser-welded was 23.1 mm in diameter. Prior to welding the foils, type-K thermocouples were placed in each one of the four holes in the sample holder. Figure 2 shows photographs of sample holders with and without welded foil samples.

During exposure tests, the sample holders were subjected to a constant pressure of 60 psi (0.41 MPa) to reproduce the state of stress that recuperator cells experience during normal microturbine operation. This pressure corresponds to the difference between the pressure of compressed air on one side of the cell and the pressure of the exhaust gases on the other. The pressure inside the sample holder is controlled using a computerized system for the duration of the test. This system also provides the means for determining whether an increase in volume in the sample holder has occurred, which would be associated with creep deformation or rupture of the foils has occurred.

During exposure tests, the sample holders are subjected to a temperature gradient as illustrated by the temperature profile depicted in Figure 3, which is for a nominal TET value of 800°C. For this case the temperature along the length of the sample holder varies between 650°C and 760°C. The temperature gradient, which results from the configuration of the microturbine, allows for the evaluation of materials over a wide range of temperatures during the same test. Table I summarizes the microturbine settings used for the test.

The material investigated in this study included alloys HR-120® and 230® alloy. These are chromia-forming austenitic nickel-based alloys developed by Haynes International Inc. Tables II and III list the composition of these alloys and the thickness of the foils that were evaluated in this study.

Figures 4 and 5 show backscattered scanning electron (BSE) images of cross-sections of foils of alloys HR120® and 230®. The presence of tungsten carbide particles in alloy 230® is evident in the micrographs in Figure 4. It can also be observed that the smaller tungsten carbide particles tend to be aligned along planes parallel to the rolling direction.

The baseline mechanical properties of the materials investigated in this study were determined at ambient temperature. Miniature dog-bone shaped tensile specimens were obtained by electron discharge machining from foils 20.3 cm wide. Test specimens were obtained with their main axis either parallel or perpendicular to the rolling direction. The dimensions of the dog-bone shaped miniature tensile specimens were 10 mm long, with a gauge section 1.27-mm wide and 3.8-mm long. Figure 6 shows a typical test specimen. The tensile stress-strain behavior of the miniature test specimens was determined under a constant crosshead displacement rate of 0.01 mm/min using an electromechanical testing machine. A special set of grips and alignment fixture were used to transfer the load to the test specimens and to ensure alignment to eliminate spurious bending strains. Because of the small dimensions of the test specimens it was not possible to determine the strain directly. However, the tensile strain of the test specimens was estimated after correcting the recorded crosshead displacement from the contribution of the machine compliance to the recorded displacement. Values for the 0.2% yield stress, ultimate tensile strength and strain failure were obtained from each stress-strain curve. These results are listed in Table IV. Data reported by the material manufacturer are listed in Table V.

At the end of 500-hr exposure tests the sample holders were removed from the microturbine, and the foils were cut from the sample holder. Miniature tensile test specimens were obtained from the foils by electron discharge machining. Other pieces of the foil were used for microstructural characterization and compositional analysis using an electron-probe microanalyzer (EPMA). While special precautions were taken to preserve the integrity of the oxide scale that formed on the surface of the foils evaluated, it was not possible to know if any material had spalled off prior to the removal of the sample holders from the microturbine.

RESULTS AND DISCUSSION

Alloy 230®

Figure 7 presents a picture of the sample holder with alloy 230® foils at the end of the 500-hr exposure test. Under regular lighting conditions the foils had a dull appearance and grew darker with exposure temperature. There was no evidence of creep deformation, in contrast to the ballooning experienced by foils of 347 stainless steel exposed to similar conditions [5].

Figure 8 presents scanning electron micrographs of the cross-sections of foils that had been exposed for 500 hours. For the case of the foil exposed at 752°C, which was located in position 1 of the sample holder, it was found that only a very thin layer of chromium oxide was present on the surface (Figure 8d). It was also found that a series of intergranular cracks, which were several micrometers long and had spanned more than one grain, had developed on the side of the foil that had been exposed to the microturbine exhaust gases. Smaller cracks were also observed on the surface of the foils that had been exposed to compressed air. Similar to the foil that had

been exposed to the highest temperature (752°C), short cracks had formed along the grain boundaries on the surface of foils that had been exposed to the microturbine exhaust gases at lower temperatures (736°C, 700°C and 679°C). Figures 8a to 8c depict scanning electron micrographs of the cross-section of these foils. Smaller cracks were also found to form on the surface that had been exposed to compressed plant air. Elemental maps (Figure 9), obtained from foils exposed to 752°C and depicted in Figure 8, showed that the surfaces of those cracks were rich in oxygen and deficient in chromium. The depletion of chromium from the grain boundaries of the base metal near the surface is evident in the elemental maps obtained. It is believed that the sub-surface degradation and cracking of the material resulted from Cr depletion and precipitation of Cr-rich carbides. Similar observations have been reported by Gleeson and Harper reported for 230® alloy after cyclic oxidation for 720 days at 982°C [6].

Figure 10 presents the stress versus strain curves from the tensile evaluation of miniature test specimens obtained from the foil at location 1 (752°C) of the sample holder. Also included are stress-strain curves for the as-received material. It was found that the ultimate tensile strength and ductility of 230® alloy decreased by 30% and 60%, respectively, after 500 hours exposure at 752°C. At the lowest exposure temperature of 679°C the ultimate tensile strength and ductility decreased by 10% and 25%, respectively. Table VI summarizes the tensile results.

The loss of ductility of 230® alloy after exposure to microturbine exhaust gases is most likely the result of carbide precipitation. Storey et al. reported that the precipitation of large M_6C carbides and smaller grain boundary $M_{23}C_6$ precipitates were responsible for the 30% decrease in ductility experienced by alloy 230® after 1500-hour long exposures at 760°C [7]. These authors also reported that a heat treatment at 1177°C for 3 hours was sufficient to re-dissolve the embrittling phases without grain growth and to restore as-processed ductility values.

The relationship in Equation 1 was found to provide a good representation of the ultimate tensile strength of alloy 230® foils as a function of 500-hr exposure temperature in ORNL's microturbine.

$$\frac{\sigma}{\sigma_o} = 1 - \left(\frac{T}{900}\right)^{7.5} \qquad (1)$$

where σ is the ultimate tensile strength at the exposure temperature T (in degrees Celsius) and σ_o is the tensile strength at 20°C.

Alloy HR-120®

Figure 11 shows the sample holder with HR-120® alloy foils at the end of the 500-hr exposure in ORNL's microturbine. Under regular lighting conditions the appearance of the foils in locations 2, 3 and 4 of the sample holder was "shiny" and brass-looking. The foil that had been exposed to the highest temperature had a dark, dull appearance.

Figure 12 presents BSE images of cross-sections obtained from HR-120® alloy foils after 500-hr microturbine exposure. A thin multiphase oxide scale had formed and it was thicker on the surface exposed to the exhaust gases. An elemental compositional map (Figure 13) revealed that the grain boundaries closest to the surface and just below the surface exposed to the exhaust gases had been depleted of chromium and enriched in nickel. In the case of HR-120® alloy foils, the oxide scale possesses a multilayered structure consisting of mixed oxides of silicon, chromium and iron.

Gleeson and Harper reported that a Si-rich oxide scale formed on HR-120® alloy after cycling oxidation for 720 days in air at 982°C [6]. They also reported the depletion of chromium in the base metal near the surface and the formation of scales containing Cr_2O_3+$NiCr_2O_4$ and NiO after thermal cycling at temperatures above 1093°C. At temperatures above 1200°C, they reported the presence of a fast-growing Fe_3O_4 oxide.

Figure 14 presents the stress versus strain curves obtained from the tensile evaluation of the miniature test specimens of HR-120® alloy before and after 500-hr long exposure in ORNL's microturbine recuperator testing facility. It was found that the ultimate tensile strength and ductility of the HR-120® alloy decreased by 15% and 50%, respectively, after exposure at 745°C. At the lowest exposure temperature of 632°C the ultimate tensile strength and ductility decreased by 10% and 23%, respectively. Table VII summarizes the tensile results.

The temperature dependence of the ultimate tensile strength for the HR-120® alloy after 500-hr exposure in ORNL's microturbine was found to be well described by Equation 2:

$$\frac{\sigma}{\sigma_o} = 1 - \left(\frac{T}{1000}\right)^{6} \qquad (2)$$

Preliminary analyses of the behavior of alloy HR-120® suggest that the decrease in ductility after exposure in microturbine results from the precipitation of Cr-rich ($M_{23}C_6$) carbides [8].

Figure 15 compares the effect of temperature of exposure in ORNL's microturbine recuperator testing on the tensile strength of 347 stainless steel and alloys 230® and HR-120®. It was found that among the three alloys, HR-120® exhibits the best retention of tensile strength, followed by alloy 230® and 347 stainless steel. Equation (3) was found to describe well the temperature dependence of the ultimate tensile strength of 347 stainless steel after a 500-hr long exposure [5].

$$\frac{\sigma}{\sigma_o} = 1 - \left(\frac{T}{825}\right)^{9.4} \qquad (3)$$

While there are no fundamental basis behind the form of the correlations in Equations 1-3, it is interesting to observe that a larger denominator and a smaller exponent are associated with increasing resistance to exposure to microturbine exhaust gases. These correlations are plotted, along with the experimental results in Figure 15. A detailed analysis of the effect of exposure to microturbine exhaust gases on the

properties and microstructure of 347 stainless steel can be found elsewhere [5].

SUMMARY

A test facility for screening and evaluating candidate materials for the next generation of microturbine recuperators has been designed and is operational at Oak Ridge National Laboratory. The core of the test facility is a 60kW Capstone microturbine, which was modified to operate at higher turbine exit temperatures and to allow the placement of test specimens at the entrance of its radial recuperator. Sample holders have been designed and instrumented to allow for the continuous recording of the temperature of the thin metallic foil test specimens and to subject these to mechanical stresses through the internal pressurization of the sample holder. Materials under evaluation are welded to the sample holder using laser or e-beam techniques and allow for the identification of potential problems in manufacturability.

Results have been presented from the evaluation of 89-μm and 102-μm thick foils of alloys 230® and HR-120®. It was found that the ultimate tensile strength and ductility of alloy 230® decreased by 30% and 60%, respectively, after 500 hours exposure at 752°C. At the lowest exposure temperature of 679°C the ultimate tensile strength and ductility decreased by 10% and 25%, respectively. Alloy 230® experienced cracking on the surface exposed to the microturbine exhaust gases and the length of those cracks grew with exposure temperature. The grain boundaries in the base metal near the surface were found to be depleted of chromium.

The ultimate tensile strength and ductility of HR-120® alloy decreased by 15% and 50%, respectively, after 500 hours exposure at 745°C. At the lowest exposure temperature of 632°C the ultimate tensile strength and ductility decreased by 10% and 23%, respectively. A layered scale comprised of oxides of nickel, chromium, iron and silicon were found to have formed on the surface of HR-120® alloy foils that were exposed to the microturbine exhaust gases. While silicon was found to be present both inside grains and at grain boundaries, it was found that grain boundaries near the interface between the base metal and the oxide scale had been depleted of chromium. Alloy HR-120® was found to exhibit the greatest resistance to exposure to microturbine exhaust gases, followed by alloy 230® and 347 stainless steel.

ACKNOWLEDGMENTS

Research sponsored by the U.S. Department of Energy, Assistant Secretary for Energy Efficiency and Renewable Energy, Distributed Energy Program, as part of the Advanced Microturbine Program, under contract DE-AC05-00OR22725 with UT-Battelle, LLC. The contributions from Mr. Randy Parten are greatly appreciated.

REFERENCES

1. "Advanced Microturbine Systems Program, Plan For Fiscal Years 2000 Through 2006," U.S. Department of Energy, Office of Energy Efficiency and Renewable Energy, Office of Power Technologies. March 2000.
2. C. F. McDonald, "Heat Recovery Exchanger Technology for Very Small Gas Turbines," Intl. Journal of Turbo and Jet Engines," vol. 13 (1966) pp. 239-261.
3. O. O. Omatete, P. J. Maziasz, B. A. Pint, and D. P. Stinton, "Assessment of Recuperator Materials for Microturbines," ORNL/TM-2000-304.
4. Lara-Curzio, E., Maziasz, P. J., Pint, B. A., Stewart, M., Hamrin, D., Lipovich, N. and DeMore, D., 2002, "Test Facility for Screening and Evaluating Candidate Materials for Advanced Microturbine Recuperators," ASME Paper #2002-GT-30581, presented at the International Gas Turbine & Aeroengine Congress & Exhibition, Amsterdam, Netherlands, June 3-6, 2002.
5. E. Lara-Curzio, R. M. Trejo, K. L. More, P. J. Maziasz, and B. A. Pint, "Screening and Evaluation of Materials for Advanced Microturbine Recuperators," Proceedings of ASME Turbo Expo 2004, June 14-17, 2004 Vienna, Austria, Paper GT-2004-54255.
6. B. Gleeson and M. A. Harper, "The Long-Term, Cyclic-Oxidation Behavior of Selected Chromia-Forming Alloys," Oxidation of Metals, **vol. 49**, Nos. 314 (1998) pp. 373-399
7. I. J. Storey, D. L. Klarstrom, G. L. Hoback, V. R. Ishwar and J. I. Qureshi, "The Metallurgical Background to Rejuvenation Heat Treatments and Weld Reparability Procedures for Gas Turbine Sheet Metal Components," *Materials at High Temperatures* **18** (4) pp. 241-247 (2001)
8. P. J. Maziasz, John P. Shingledecker, Bruce A. Pint, Neal D. Evans, Y. Yamamoto, K. L. More and E. Lara-Curzio, "Overview Of Creep Strength And Oxidation Of Heat-Resistant Alloy Sheets And Foils For Compact Heat-Exchangers," Proceedings of ASME Turbo Expo 2005, June 6-9, 2005, Reno, Nevada, Paper GT2005-68927

Table I. Microturbine settings for 500-hr test.

Engine Speed	45,000 RPM
Turbine Exit Temperature	800°C
Sample holder pressure	60 psi
Fuel	natural gas

Table II. Composition of 230® alloy (wt. %)
(Haynes International, Kokomo, IN 46904)

Element	Concentration	Element	Concentration	Element	Concentration
Ni	57 (balance)	Mo	2	Al	0.3
Cr	22	Mn	0.5	C	0.1
W	14	Si	0.4	La	0.02
Co	5 (max)	Fe	3 (max)	B	0.015 (max)

Table III. Composition of HR-120® alloy (wt. %)
(Haynes International, Kokomo, IN 46904)

Element	Concentration	Element	Concentration	Element	Concentration
Ni	37	Mo	2.5 (max)	Al	0.1
Cr	25	Mn	0.7	C	0.05
W	2.5 (max)	Si	0.6	Cb	0.7
Co	3 (max)	Fe	33 (balance)	B	0.004
N	0.2				

Table IV. Summary of tensile results for as-received materials. Values correspond to mean values ± one standard deviation.

230® alloy	0.2% Yield Strength (MPa)	Ultimate Tensile Strength (MPa)	Failure Strain (%)
0.089-mm thick			
⊥ to rolling direction	452± 24	780 ± 18	36 ± 4
∥ to rolling direction	422 ± 12	770 ± 11	34 ± 2
0.102-mm thick			
⊥ to rolling direction	466 ± 23	817 ± 12	40 ± 4
∥ to rolling direction	489 ± 45	818 ± 27	36 ± 3
HR-120® alloy			
0.089-mm thick			
∥ to rolling direction	373 ± 31	697 ± 4	37 ± 5

Table V. Tensile Properties of 230® alloy (hot-rolled and 1232°C solution annealed plate) and alloy HR-120® (solution heat-treated plate)
(Haynes International, Kokomo, IN 46904)

	Yield strength at 0.2% Offset (MPa)	Tensile strength (MPa)	Elongation (%)
230® alloy	375	840	48
HR-120® alloy	375	735	50

Table VI. Summary of tensile results for 230® alloy. Values correspond to mean values ± one standard deviation.

Foil	Thickness (mm)	T (°C)	0.2% σ_y (MPa)	UTS (MPa)	Failure strain (%)
1	0.089	752	415 ± 12	561 ± 28	13.0 ± 3.0
2	0.102	736	457 ± 15	660 ± 34	19.0 ± 3.4
3	0.089	700	418 ± 41	644 ± 24	19.0 ± 2.9
4	0.102	679	481 ± 7.1	728 ± 22	27.0 ± 6.3

Table VII. Summary of tensile results for HR-120® alloy. Values correspond to mean values ± one standard deviation.

Foil	T (°C)	0.2% σ_y (MPa)	UTS (MPa)	Failure strain (%)
1	745	388 ± 35	594 ± 32	18.0 ± 4.4
2	730	421 ± 37	615 ± 30	21.0 ± 4.4
3	700	408 ± 39	582 ± 48	23.0 ± 4.7
4	632	407 ± 27	631 ± 53	29.0 ± 4.7

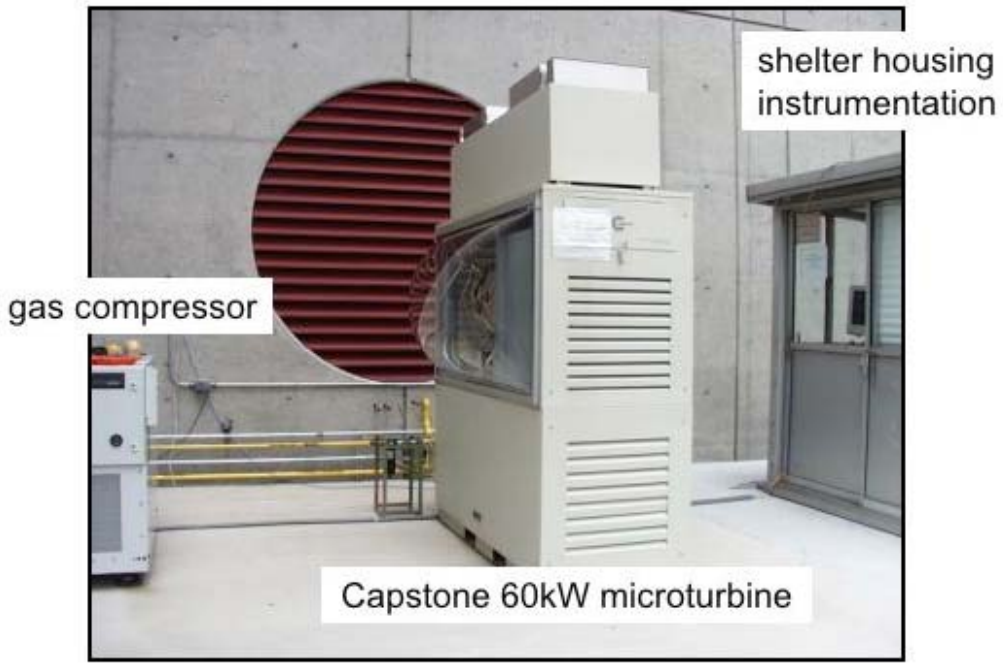

(a)

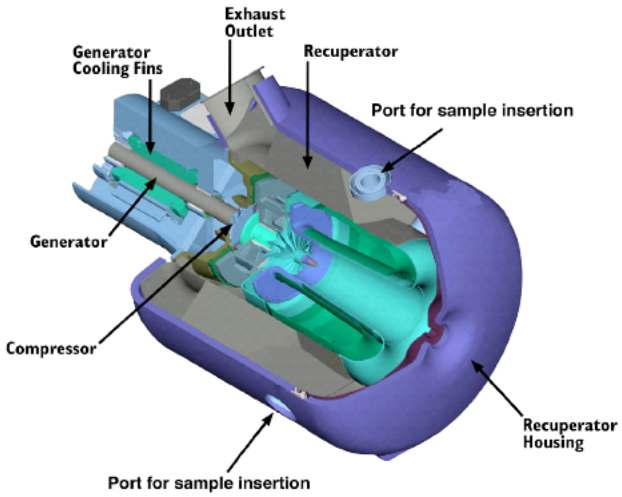

(b)

Figure 1. (a) ORNL's microturbine recuperator testing facility. (b) Schematic of modified 60kW Capstone microturbine. Note location of port bosses for placement of test specimens at the entrance of the radial recuperator.

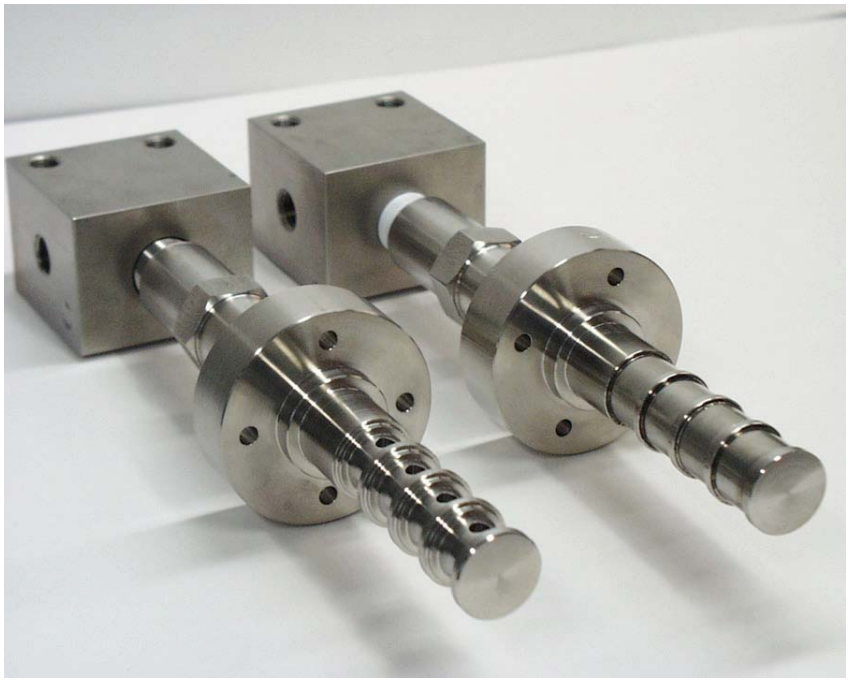

Figure 2. Sample holders for exposure of metallic foils in ORNL's microturbine recuperator testing facility. The orifices where thermocouples are placed and that are used to allow mechanical stressing of test specimens through pressurization is shown on the left. A sample holder with laser-welded metallic foils is shown on the right.

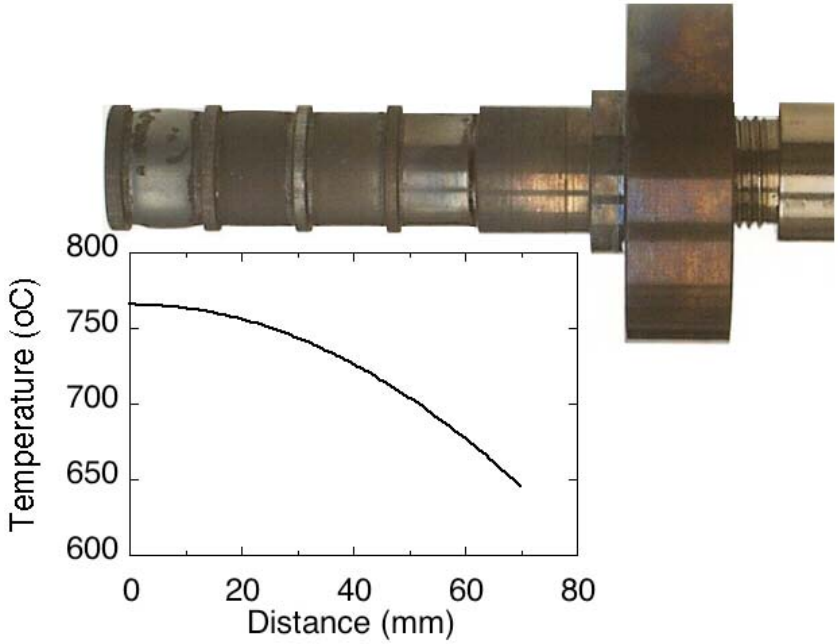

Figure 3. Temperature distribution along sample holder for a TET =800°C.

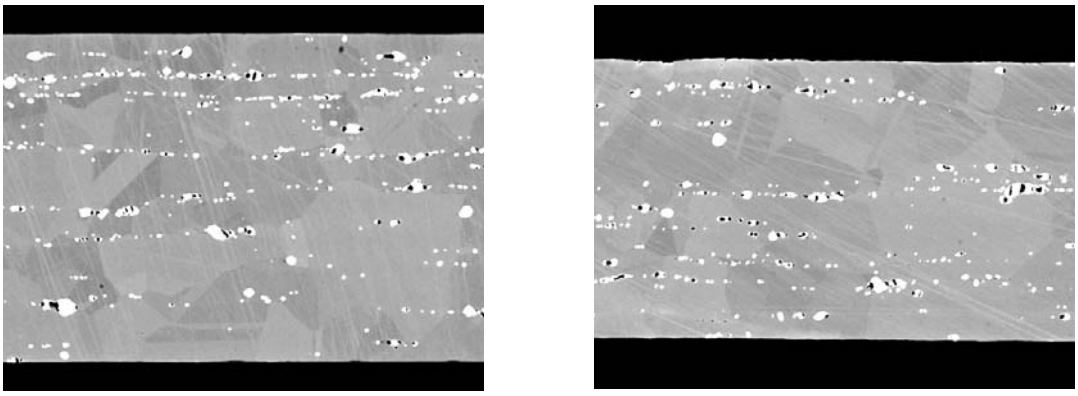

(a) (b)

Figure 4. BSE image of (a) 89-μm and (b) 102-μm thick foils of 230® alloy. Grain structure and large W-rich particles (bright particles) are clearly visible. Voids inside W-rich particles likely form during polishing.

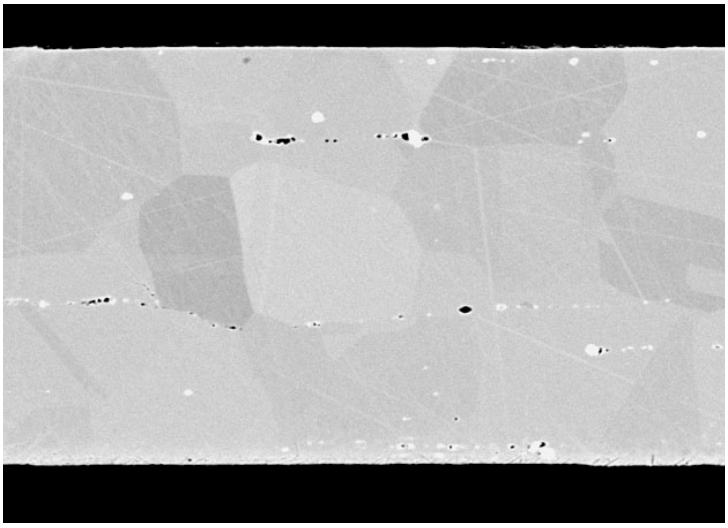

Figure 5. BSE image of 89-μm thick foil of HR-120®. The grain structure and large Nb-rich particles (bright white) are clearly visible

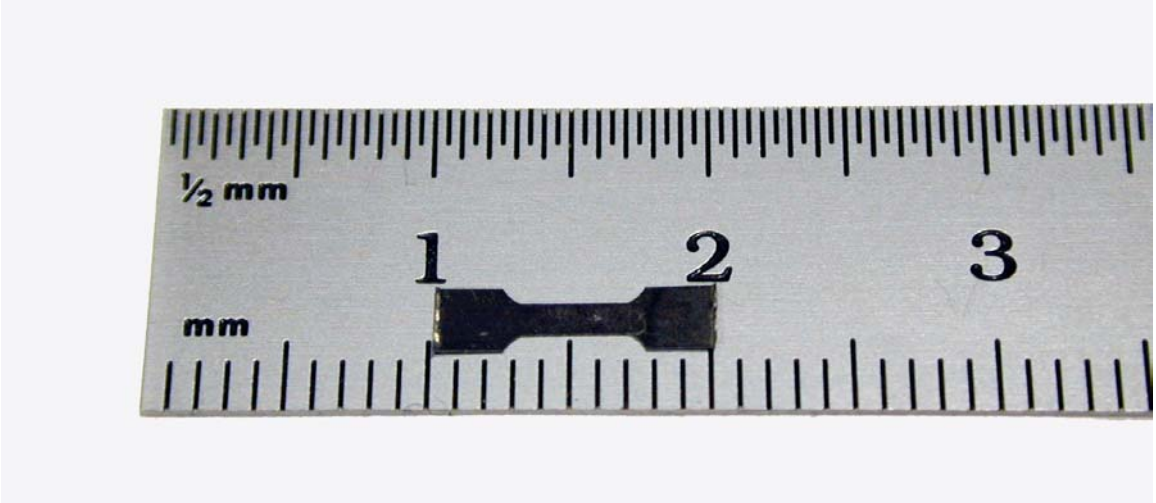

Figure 6. Miniature tensile test specimen for evaluation of mechanical properties of metallic foils. Tests specimens are obtained by electron-discharge machining.

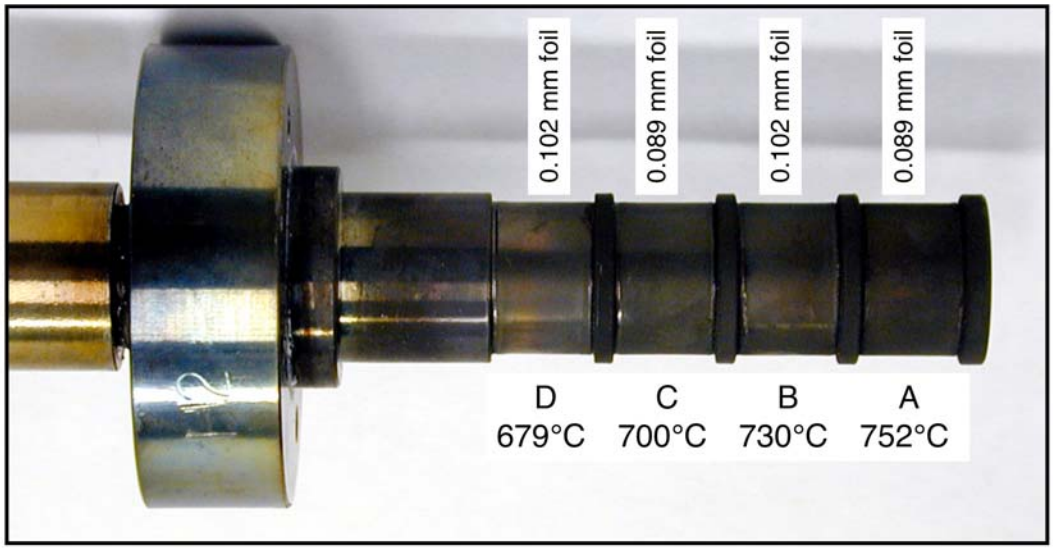

Figure 7. Sample holder with 230® alloy foils after 500-hr exposure in ORNL's microturbine recuperator testing facility at TET=800°C.

exhaust gas surface

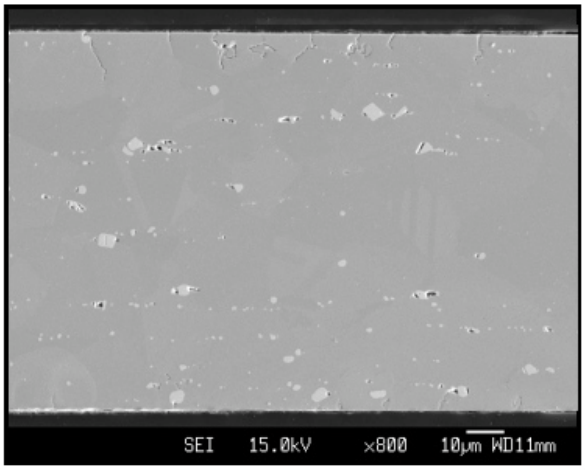

(a) 679°C

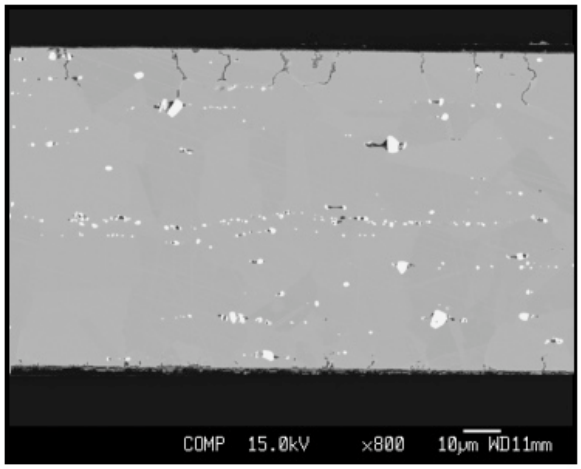

(b) 700°C

exhaust gas surface

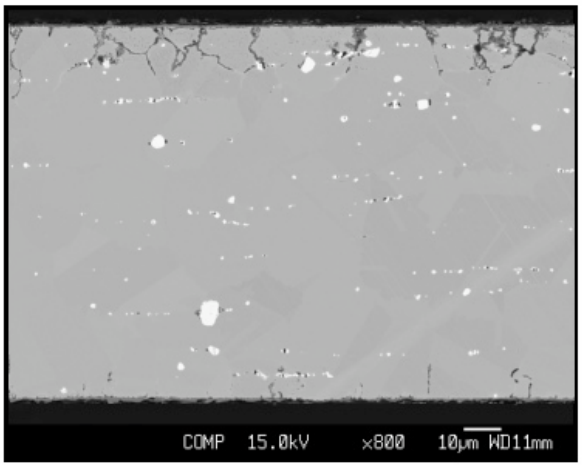

(c) 736°C

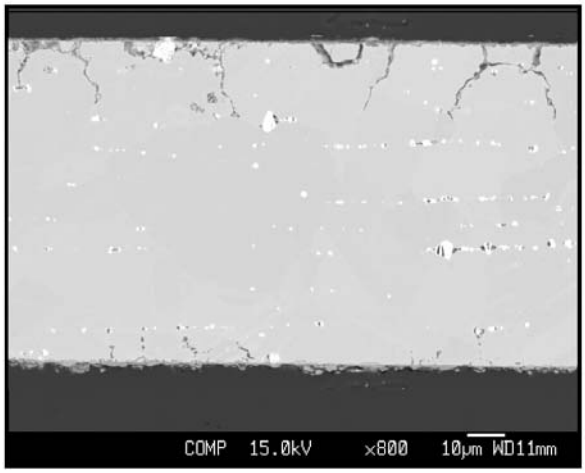

(d) 752°C

Figure 8. BSE images of 230® alloy: (a) 89-μm thick foil; (b) 102-μm thick foil; (c) 89-μm thick foil; (d) 102-μm thick foil.

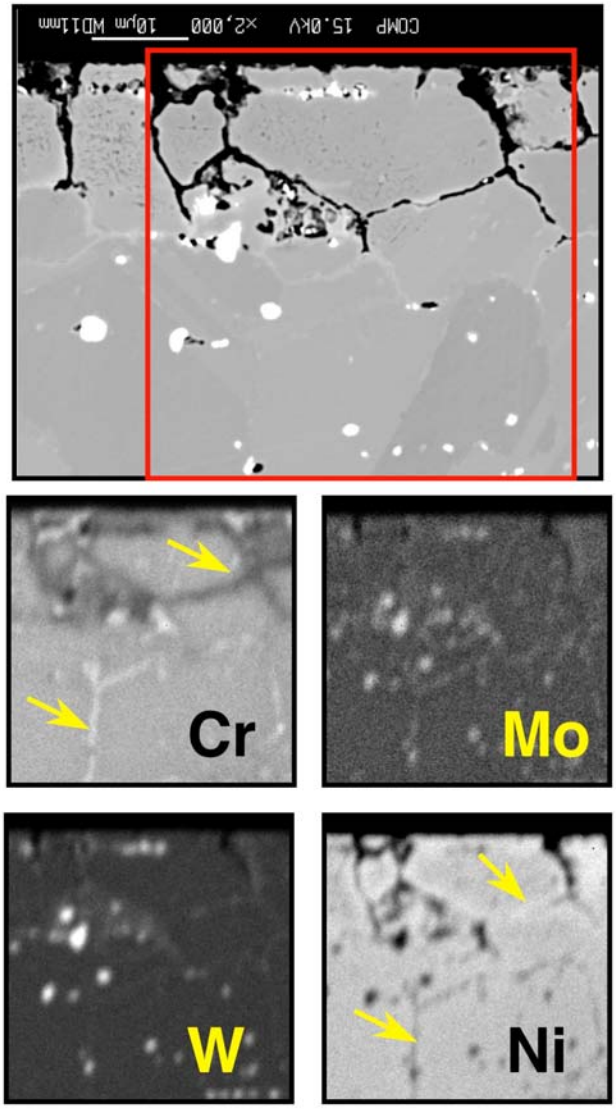

Figure 9. BSE image and corresponding elemental maps obtained from a 89-μm thick foil of 230® alloy after a 500-hr long exposure at 752°C in ORNL's microturbine recuperator testing facility. Surface at the top of the micrographs had been exposed to the microturbine exhaust gases. Note the depletion of chromium along the grain boundaries near the surface. Grain boundaries in the bulk are rich in chromium and Ni-depleted.

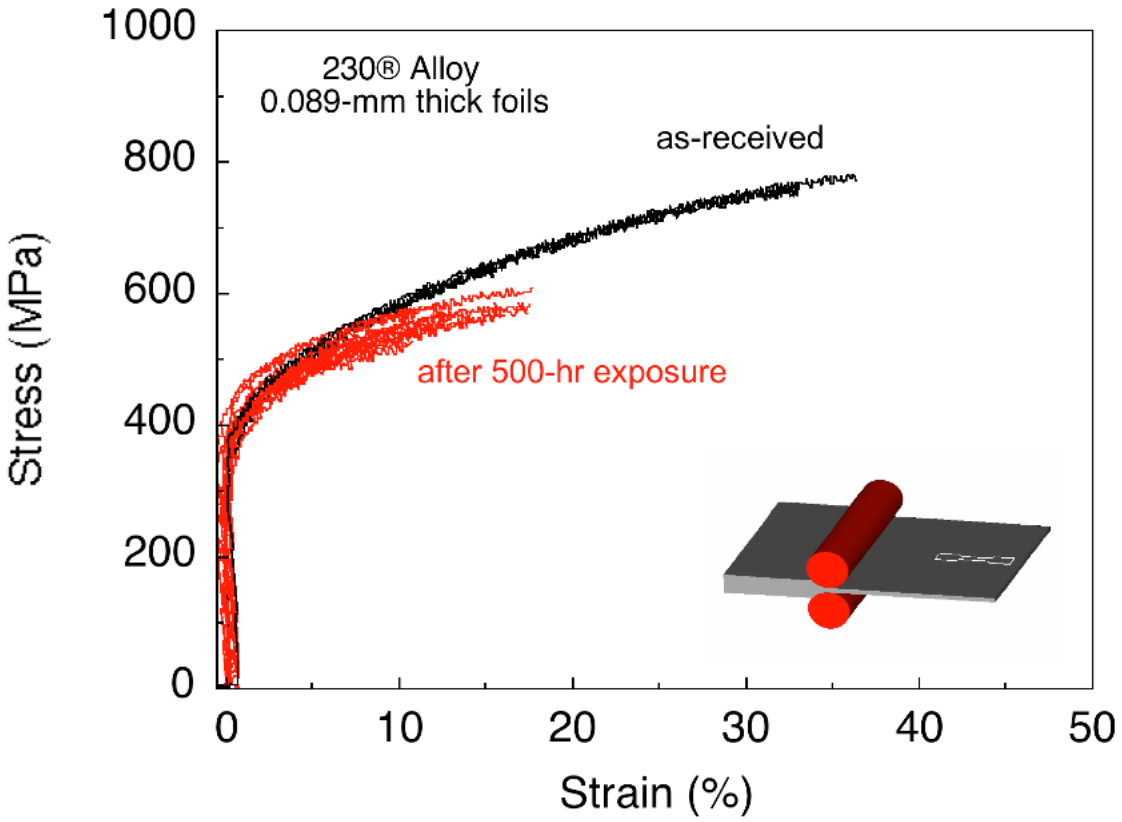

Figure 10. Tensile stress-strain results obtained from the evaluation of miniature tensile specimens of 89-μm thick foils of 230® alloy before and after 500-hr exposure in ORNL's microturbine recuperator testing facility at 752°C.

Figure 11. Sample holder with HR120® alloy foils after 500-hr exposure in ORNL's microturbine recuperator testing facility at TET=800°C.

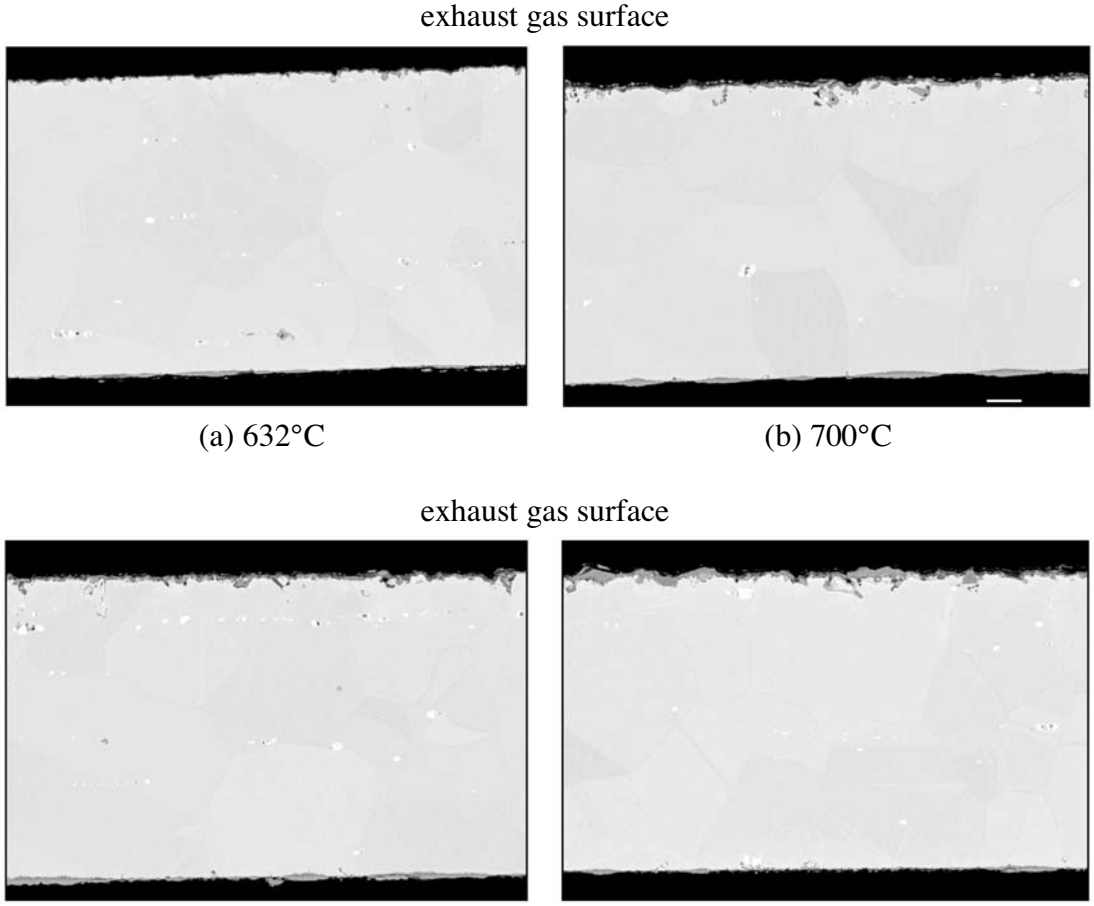

(a) 632°C (b) 700°C

(c) 730°C (d) 745°C

Figure 12. BSE images of cross-sections obtained from 89-μm thick HR-120® alloy foils after 500-hr exposure at TET=800°C. The upper surface in the micrograph had been exposed to the microturbine exhaust gases.

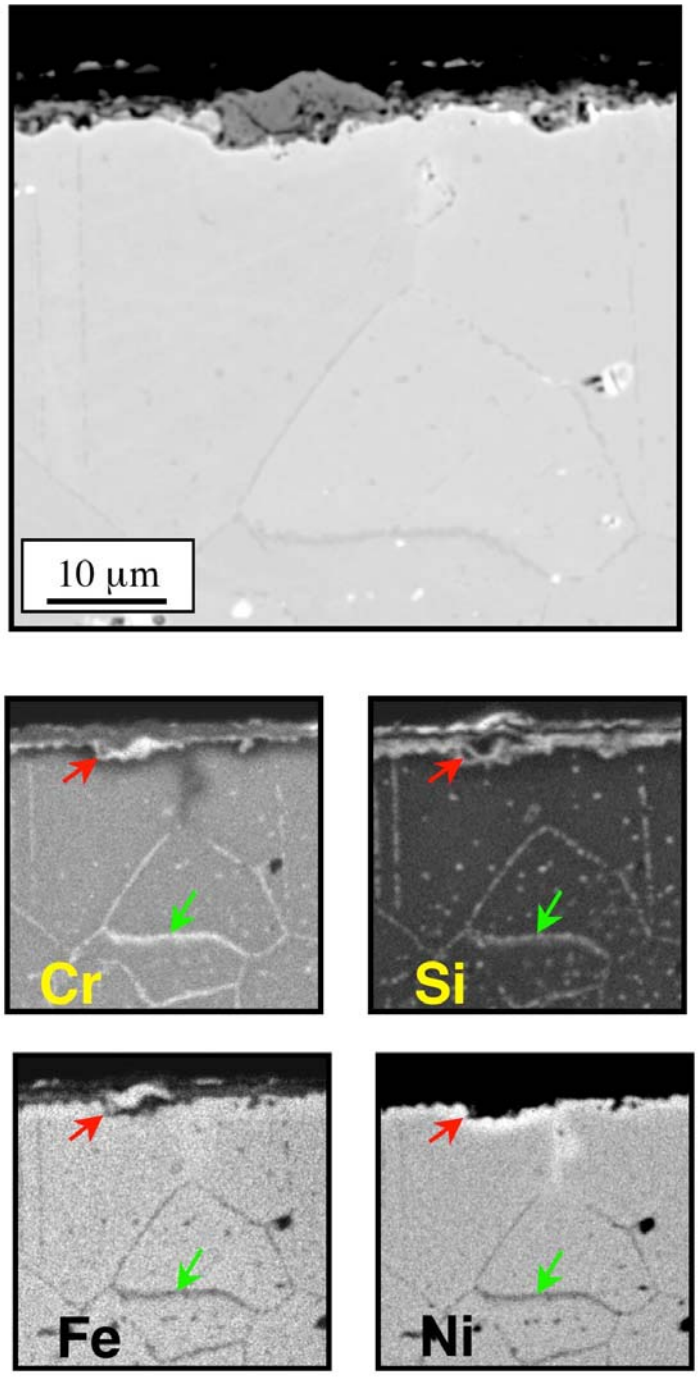

Figure 13. BSE image and corresponding elemental maps from cross-sectional area of 89-μm thick HR-120® alloy foil that was exposed for 500 hours at 745°C. The upper surface in the micrograph had been exposed to the microturbine exhaust gases. Note that the grain boundaries near the surface are poor in chromium but rich in nickel.

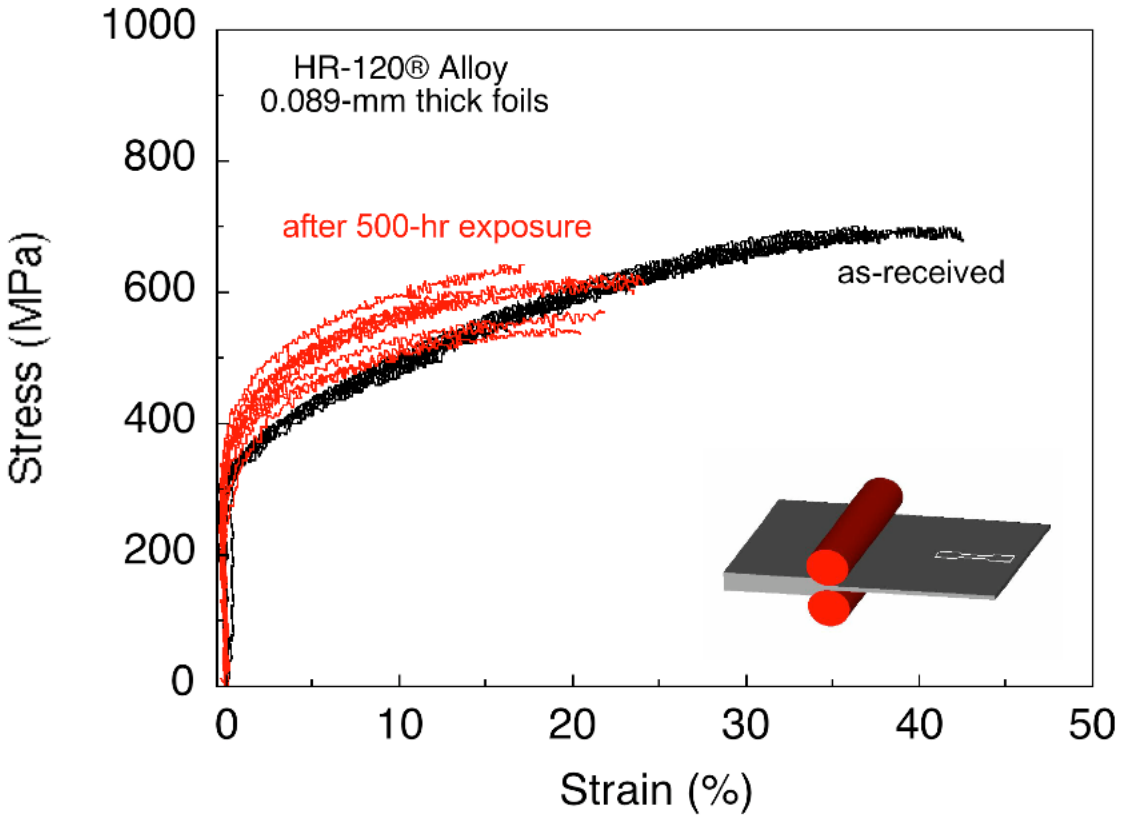

Figure 14. Tensile stress-strain results obtained from the evaluation of miniature tensile specimens of 89-μm thick foils of HR-120® alloy before and after 500-hr exposure in ORNL's microturbine recuperator testing facility at 745°C.

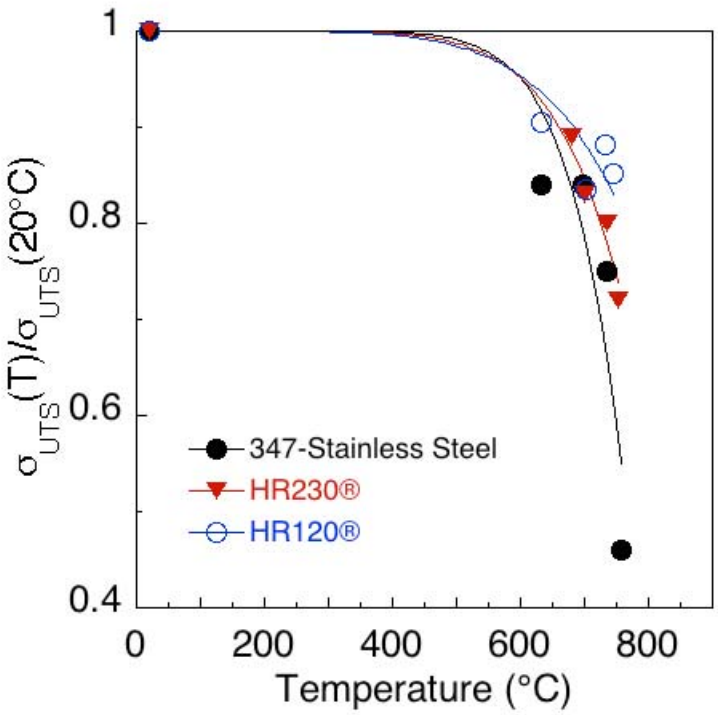

Figure 15. Effect of temperature on the ultimate tensile strength of 347 stainless steel and alloys 230® and HR-120® after 500-hr exposure in ORNL's microturbine recuperator testing facility.